A Simulation-Based Approach for the Automated Design of Fatigue Resistant Continuous Fibre-Reinforced Components

Marc Gadinger[1,*], Christoph Bode[1], Torben Deutschmann[2], Dieter Krause[2], Sandro Wartzack[1]

[1] Friedrich-Alexander-Universität Erlangen-Nürnberg, Engineering Design, Martensstr. 9, 91058 Erlangen, Germany
[2] Hamburg University of Technology, Institute of Product Development and Mechanical Engineering Design, Denickestr. 17, 21073 Hamburg, Germany

** Corresponding author:*
Marc Gadinger
Friedrich-Alexander-Universität Erlangen-Nürnberg
Engineering Design
Martensstr. 9
☎ *+49 9131/85 23 215*
✉ *gadinger@mfk.fau.de*

Abstract

Fibre-reinforced plastics are increasingly being used in important structural components. Here they are often subjected to cyclic loading, which leads to a deterioration in material properties. However current design methods hardly take this fatigue behavior into account. Instead, they rely on conservative safety factors, resulting in over-dimensioned components. In order to realise the full lightweight potential, we propose an innovative method that enables a targeted design for a defined service life. It integrates knowledge from experimental fatigue testing and uses modified mathematical failure criteria to predict the degree of fatigue throughout the part. This allows us to adaptively reinforce fatigue critical areas, resulting in lightweight and fatigue resistant structures.

Keywords

fatigue behavior, fibre-reinforced plastics, lightweight design, optimization

 | DOI: 10.35199/dfx2024.10

1. Motivation

Lightweight design and the efficient use of materials are becoming a major focus in various economic sectors. This is also evident from upcoming leading initiatives and legal requirements in the context of climate goals and the transition to a more resource-efficient economy. Components made from fibre-reinforced plastics (FRPs) are therefore increasingly used as important structural parts in series production. There, they are often subjected to cyclic loading, which, with an increasing number of cycles, lead to a deterioration or degradation of the material properties due to the formation and propagation of microcracks [1, 2]. However, current design approaches and optimization routines hardly take this fatigue behavior into account. Instead, over-dimensioning based on empirical criteria is often employed. To fully exploit the lightweight potential of FRP components, a targeted design for a defined service life is more effective.

2. State of the Art

FRPs offer significant potential for lightweight applications, but they also exhibit very complex fatigue behaviour. During fatigue processes in FRPs, a specific combination of damage occurs, affecting the fibres, the matrix and the interfaces. Additionally, local debonding and large-scale delamination occurs. This interplay of various factors results in a very complex damage pattern.

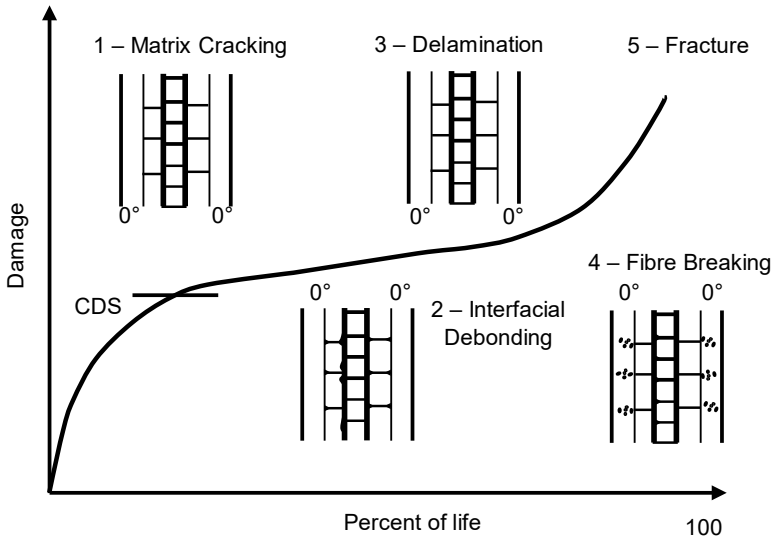

Figure 1: Progress of fatigue damage in FRPs according to [1].

Over the lifespan of FRPs, these effects lead to a loss of stiffness, which is often quantified by a damage factor. The loss of stiffness is depicted in Figure 1 and can be divided into three phases. The first phase is characterized by a significant reduction in material stiffness due to crack formation in the matrix. In the second phase, the extent of damage continues to increase, but at a slower rate than in phase one. In the final phase, the damage sharply increases again due to local failures caused by fibre breakage or complete delamination of the interfaces [1, 2].

The basis for understanding the fatigue behavior of FRPs are experimentally determined S-N curves [3, 4]. For this purpose, test specimens are cyclically loaded at a constant load ratio until failure. Equation 1 describes the course of such a fatigue curve. Using the slope parameter b and the strength parameter R, the maximum tolerable stress σ_{res} for a specific number of cycles N can be determined [5].

$$\sigma_{res} = R \cdot N^{b} \quad (1)$$

Usually more than one S-N curve is needed to capture the fatigue behavior of FRPs, as it is influenced not only by the magnitude of the applied load load – but also by the orientation of the fibres relative to the direction of force, the frequency of cyclic loading and environmental conditions such as temperature and humidity [6, 7].

There are fewer approaches to the optimization of FRP structures under cyclic loading than there are for static loading. Typically, the complex fatigue behavior is addressed by applying a global safety factor within a static design or optimization process [8]. Among the limited methods for cyclic optimization is the approach by Ertas et al. [9], which optimizes existing structures by adjusting the layer sequence, layer thicknesses, and fibre orientations without adding new layers, using a lifespan prediction model by Fawaz et al. [10, 11]. Another method, proposed by Deveci et al. [12], employs a hybrid optimization approach that combines a genetic algorithm with a lifespan model – specifically the failure tensor polynomial in fatigue model – by Philippidis et al. [13], which is based on the Tsai-Han failure criterion [14]. Both approaches demonstrate that a failure criterion combined with S-N curves can produce accurate lifespan predictions which can be used to optimize FRP-components against cyclic loading conditions. However, the present methods are computationally intensive, as the optimization process can take up to 1000 generations.

3. Research Problem and Research Goal

The traditional approach to designing dynamically loaded structures involves incorporating a safety factor into an otherwise static design. However, this approach does not adequately address the complex fatigue behavior of FRPs and is extremely inefficient in terms of the resulting weight [3]. Although few methods exist for optimizing FRPs under cyclic loading, they involve significant computational effort and mostly focus on refining the existing structure. A promising advancement for continuous fibre-reinforced composites is Fibre-Patch-Placement (FPP), which involves the automated application of unidirectional fibre-reinforced strips to an existing base laminate. This technique allows for precise reinforcement of components along existing load paths [4]. Integrating the advancements in FPP into the optimization of dynamically loaded structures could yield significant benefits.

The central research questions of this work are therefore: How can components made of FRPs be optimized as mass-efficiently as possible against fatigue damage due to cyclic loading? Specifically, is it possible to develop a design method that ensures the achievement of a required minimum number of cycles through the use of local reinforcements on a base laminate?

4. Methods and Procedures

4.1. Overview

The basic procedure of the optimization method is illustrated in Figure 2. The quality criterion for the optimization is to ensure that the critical number of cycles N_{krit} – a value to be initially specified by the product developer – is reached for each element and each layer in the model. The main control variable is the application of new layers in the form of patches on an existing base laminate. During the optimization, the fibre orientations of the main layers are also refined by aligning them with the principal direction of the highest stresses. However, this adjustment is independent of the quality criterion and serves only as a secondary condition.

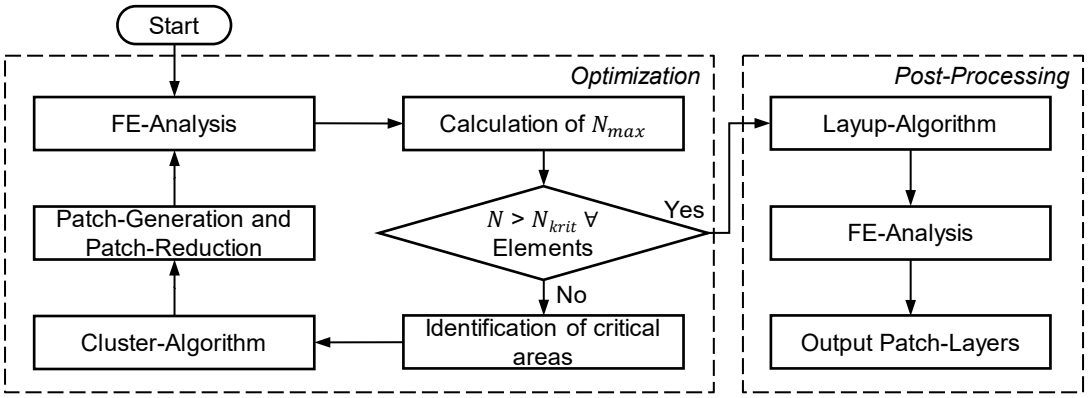

Figure 2: Process of the optimization method.

First, the FE model of the component to be analysed is imported, along with the associated boundary conditions and load cases. Using the locally resolved stresses and strains from an FE-Analysis, the maximum tolerable number of cycles is calculated for each layer in every element. The procedure for calculating the tolerable number of cycles is described in more detail in Section 4.2. Each iteration of the optimization continues with the identification of fatigue critical areas within the component. For this purpose, each element in every layer is checked for compliance with the quality criterion ($N > N_{krit}$). The algorithm stores the elements whose calculated number of cycles is less than the specified minimum value. In the subsequent step, the clustering function uses the stress states of the critical elements to determine the principial directions of the stresses. The following patch generation requires both the information from the FE-Analysis and the clustering. It converts the clusters into corresponding patches and assigns a fibre orientation to the patch according to the direction of the greatest principal stress within the cluster. Finally, a patch reduction step is carried out. In the patch-based optimization of FRP components, patches in certain regions influence the entire component through the stiffness matrix. Weak areas can thus be reinforced even without their own patch layers. Therefore, the elements that have been reinforced by patches are now checked to determine if they are stable enough to forgo the reinforcement.

As soon as all elements meet the quality criterion, the patches calculated in the optimization are converted into manufacturing-compliant unidirectional strips for the FPP process. For this purpose, a layup algorithm according to Voelkl et al. is used [15]. This algorithm considers each of the determined patches and generates a rectangular strip with a user-defined width and length adapted to the patch size. Figure 3 shows an example of how tape strips are created that fully encompass the previously determined patches.

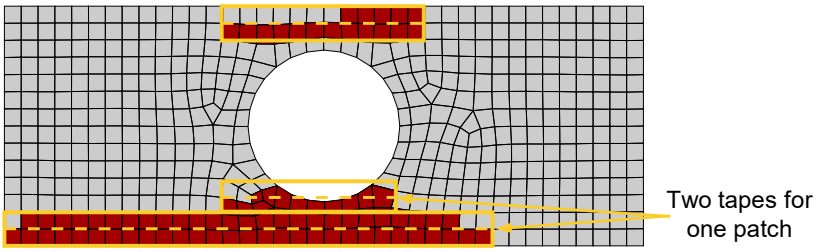

Figure 3: Exemplary representation of UD-tapes (yellow) over patch areas determined in the optimization (red) according to [15].

4.2. Determination of Maximum Tolerable Number of Load Cycles

A key aspect of the optimization process is calculating the maximum tolerable number of fatigue cycles until failure. This is achieved by determining the stresses and strains within the

component using FE-Analysis, and then resolving these locally for each layer and element with a modified failure criterion, which combines the local stress tensor components into a function indicating failure when a threshold is reached [16].

Generally, the failure of a single layer does not lead to the failure of the entire component, so criteria for single layers are usually referred to as fracture criteria. However, since this work considers the failure of the first layer significant, this distinction is not strictly necessary. A widely used model for describing the failure behavior of FRPs is the Tsai-Hill criterion. Other comparable models include the Tsai-Wu criterion and the Puck criterion, the latter being able to distinguish between fibre and inter-fibre failure [17]. In this paper, the Puck criterion is chosen for this reason and its suitability for highly anisotropic materials.

As explained in section 2, the S-N curve describes the decline in material strength with an increasing number of cycles. For FRPs, it is essential to differentiate between strengths parallel to the fibre, perpendicular to the fibre, and in the shear direction, which leads to Equations 2a-c. These equations also account for distinct strengths in compression and tension.

$$\sigma_{\parallel,res}^{+,-} = R_{\parallel}^{+,-} \cdot N^{b} \tag{2a}$$

$$\sigma_{\perp,res}^{+,-} = R_{\perp}^{+,-} \cdot N^{b} \tag{2b}$$

$$\tau_{\perp\parallel,res} = R_{\perp\parallel} \cdot N^{b} \tag{2c}$$

To achieve the most accurate predictions, the slope parameters for Equations 2a-c ideally should be determined for each stress direction and type of loading as these factors influence the fatigue behavior [18]. For simplicity in this work, b is treated as a uniform parameter across all three stress directions, derived from an S-N curve of a laminate material with layers of different orientations [19].

4.2.1. Modified Puck-Criterion for Fibre Failure

By substituting the static strengths in the Puck criterion with the corresponding S-N Equations 2a-c, the maximum sustainable number of fatigue cycles for a specific stress state can be determined. Thus, the strength in the criterion depends on the current number of cycles:

$$\left(\frac{\sigma_{\parallel}}{R_{\parallel}^{+,-} \cdot N^{b}}\right) = 1 \tag{3}$$

Rearranging Equation 3, we can determine the maximum number of cycles N_{Fb} under an applied stress $\sigma_{\parallel}$:

$$N_{Fb} = \sqrt[b]{\frac{\sigma_{\parallel}}{R_{\parallel}^{+,-}}} \tag{4}$$

4.2.2. Modified Puck-Criterion for Inter-Fibre Failure

Inter-fibre failure is differentiated into three modes, with auxiliary equations determining the applicable mode. Since all strengths decrease with the same slope b, the auxiliary equations do not need adjustment for the change in strength. In all three modes, the resulting strength $R \cdot N^{b}$ replaces the static strength, reflected in mode A, mode B and mode C in Equations 5, 6 and 7, respectively.

$$\sqrt{\left(\frac{\tau_{\perp\parallel}}{R_{\perp\parallel} \cdot N^{b}}\right)^{2} + \left(1 - p_{\perp\parallel}^{+} \frac{R_{\perp}^{+} \cdot N^{b}}{R_{\perp\parallel} \cdot N^{b}}\right)^{2} \left(\frac{\sigma_{\perp}}{R_{\perp}^{+} \cdot N^{b}}\right)^{2}} + p_{\perp\parallel}^{+} \frac{\sigma_{\perp}}{\tau_{\perp\parallel} \cdot N^{b}} = 1 \tag{5}$$

$$\frac{1}{R_{\perp\parallel}\cdot N^b}\left(\sqrt{\sigma_{\perp\parallel}^2+(p_{\perp\parallel}^-\sigma_\perp)^2}+p_{\perp\parallel}^+\sigma_\perp\right)=1 \tag{6}$$

$$\left[\left(\frac{\tau_{\perp\parallel}}{2\left(1+p_{\perp\parallel}^-\right)R_{\perp\parallel}\cdot N^b}\right)^2+\left(\frac{\sigma_\perp}{R_\perp^-\cdot N^b}\right)^2\right]\frac{R_\perp^-\cdot N^b}{(-\sigma_\perp)}=1 \tag{7}$$

Through a transformation, equations for the maximum number of fatigue cycles N_{Zfb} as a function of stress are also derived here for mode A

$$N_{Zfb}=\sqrt[b]{\sqrt{\left(\frac{\tau_{\perp\parallel}}{R_{\perp\parallel}}\right)^2+\left(1-p_{\perp\parallel}^+\frac{R_\perp^+}{R_{\perp\parallel}}\right)^2\cdot\left(\frac{\sigma_\perp}{R_\perp^+}\right)^2}+p_{\perp\parallel}^+\frac{\sigma_\perp}{R_{\perp\parallel}}}, \tag{8}$$

for mode B

$$N_{Zfb}=\sqrt[b]{\frac{1}{R_{\perp\parallel}}\left(\sqrt{\tau_{\perp\parallel}^+{}^2+\left(p_{\perp\parallel}^-\sigma_\perp\right)^2}+p_{\perp\parallel}^-\sigma_\perp\right)} \tag{9}$$

and for mode C

$$N_{Zfb}=\sqrt[b]{\left[\left(\frac{\tau_{\perp\parallel}}{2(1+p_{\perp\parallel}^-)R_{\perp\parallel}}\right)^2+\left(\frac{\sigma_\perp}{R_\perp^-}\right)^2\right]\frac{R_\perp^-}{(-\sigma_\perp)}}. \tag{10}$$

When applying the modified Puck criterion, it is critical to consider fibre failure and inter-fibre failure independently, resulting in two maximum cycle numbers, N_{Fb} and N_{Zfb}. The algorithm then selects the smaller value that represents the critical failure case.

5. Optimization of a Curved Component under Cyclic Load

In the following section, the presented optimization method is applied to a shear panel with complex shapes, including double curvature. The geometry of the shear panel and the defined boundary conditions are shown in Figure 4. The component is rigidly fixed through the lower four holes, while the middle holes are loaded with 4000 N and the upper holes with 8000 N. This loading configuration induces tensile, compressive, and shear stresses within the component.

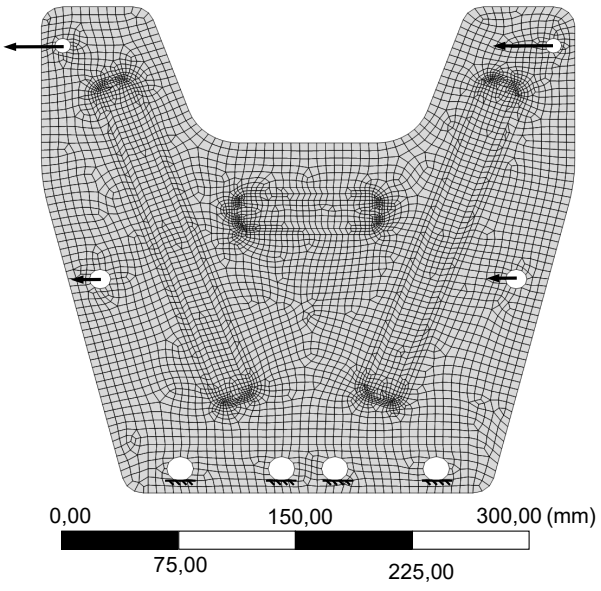

Figure 4: Representation of the geometry and the boundary conditions of the component to be optimized.

For the simulation, a unidirectional carbon fibre-reinforced epoxy resin with a symmetrical layer configuration of $[45, 90, -45, 0]_s$ was used. The material properties used in the simulation are given in Table 1. The layer thickness is set to 0.2 mm. Both the stiffeners and the clamping regions are reinforced with a thicker material. The critical number of cycles N_{krit} is set to 100,000 cycles. The allowable angular difference between the principal directions of two patches is 20°, the tape width is set at 50 mm, and the patch thickness is set to 0.6 mm.

Table 1: Properties of the laminates used in the study [19, 20].

Material properties	Strength properties	Fatigue properties
$E_{11} = 123\ \text{GPa}, E_{22} = 7.78\ \text{GPa}$	$X_t = 1632\ \text{MPa}, -X_c = 704\ \text{MPa}$	$b = -0.0711$
$G_{12} = 5\ \text{GPa}$	$Y_t = 34\ \text{MPa}, -Y_c = 68\ \text{MPa}$	
$v_{12} = 0.27$	$S_{21} = 80\ \text{MPa}$	

Figure 5 summarizes the optimization process through a series of diagrams. The first graph (a) shows the maximum tolerable number of cycles of the weakest element in each iteration. Significant fluctuations are observed, likely due to the complex stress states within the component. It can be seen how the optimization attempts to gradually approach the critical value of 100,000 cycles from above once it is exceeded. The relative weight increase in graph (b) indicates that hardly any patches are added after the tenth iteration, as can be seen from the relatively constant weight change from the tenth iteration onwards. Therefore, the fluctuations in (a) are generated by only a small fraction of the elements. The median number of cycles of the critical elements (c) also shows slight fluctuations, but with a clear upward trend.

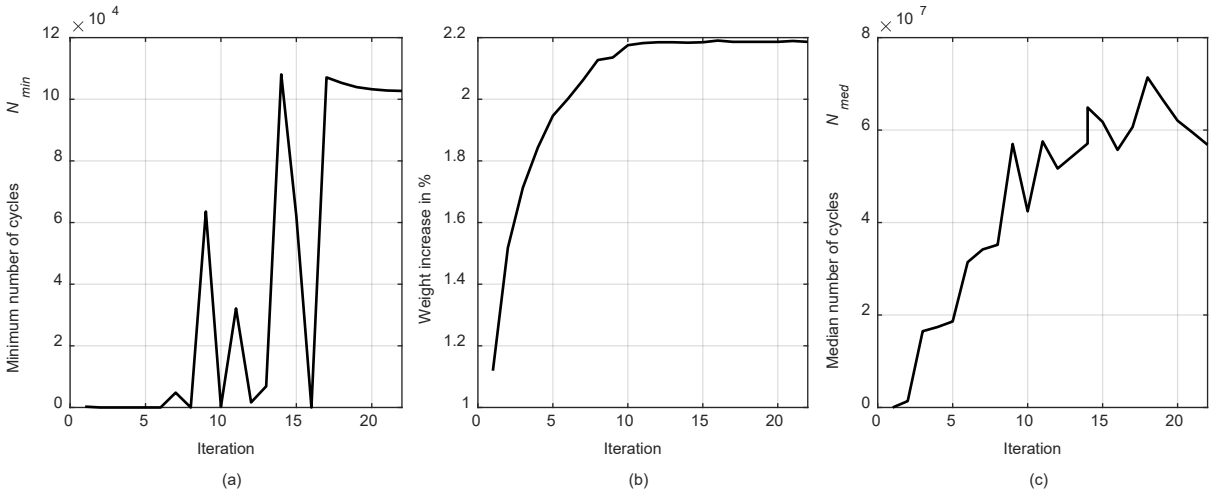

Figure 5: (a) Progression of the minimum number of cycles N_{min} of the component; (b) Progression of the weigth increase in %; (c) Progression of the median number of cycles N_{med} of all critical elements in each iteration.

After optimization, post-processing is performed, including the layup algorithm. The results are shown in Figure 6, where the central axis of each patch is indicated by yellow lines. In addition, the number of reinforcing patches is visualized by a colormap. The maximum number of layers is 12 (8 base layers + 4 patches). The left clamping hole and the tip of the right stiffener are particularly heavily reinforced with tape, as is the right mounting hole. Due to the shear load, a moment is generated in the component, with the two inner holes being closer to the neutral axis of this moment, resulting in them being less heavily loaded and thus not

reinforced. To avoid excessive thickening due to overlapping patches, it could be advisable to further consolidate adjacent and similarly long patches further.

In total, many relatively long tape strips are arranged mostly diagonally, reinforcing fatigue critical parts. For production, some of the shorter strips could potentially be further combined to increase manufacturing compliance. Overall, the fatigue strength of the demonstrator could be optimized against the applied dynamic loading conditions without significant changes to the component. Most of the component remains unchanged, as the method focused on the critical areas by applying local reinforcing tapes. Furthermore, finding the optimized design took only 23 iterations.

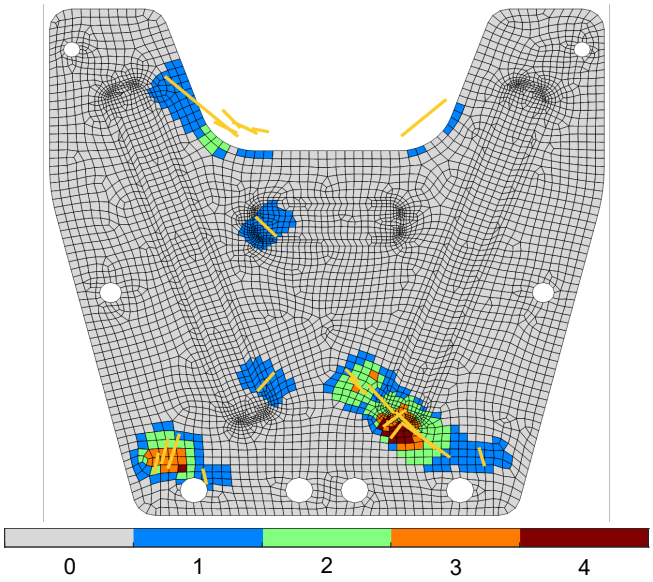

Figure 6: Number of patch layers after post-processing and centre axes of the UD-tapes.

5.1. Optimization with a Static Approach

To compare the optimization performed by the presented method with existing design methods, this section examines a static design of the same component under identical boundary conditions using a method developed by Klein called mfkCODE [21]. This method optimizes the component based on patches for an applied static load. To then adapt the static design for dynamic loading conditions, the guideline VDI 2014 [8] is applied, specifying allowable stresses in fibre orientation, transverse orientation and shear direction. Following the patch design by mfkCODE, a thickness optimization is conducted to meet these requirements.

The weight-specific number of cycles (N_{wsc}) metric is used to compare the method with the static approach. N_{wsc} is calculated as the quotient of the tolerable number of cycles and the total mass of the component, measured in cycles per gram. In this experiment, N_{wsc} for dynamic optimization is 20.81 cycles per gram, while for static optimization, it is 15.11 cycles per g. This shows a 33% improvement of the new design over the optimization using mfkCODE followed by thickness optimization after guideline VDI 2014.

To further compare the optimizations, the Puck criterion representation is used. Figure 7 shows the Puck values for the unoptimized component (a), the component after dynamic optimization (b) and after optimization with mfkCODE (c). Both optimization methods reduce the Puck values at the stress peaks. Notably, in this experiment, the optimization with the new method produces less uniform Puck values across the component. One reason could be that it focuses on relatively small areas with high stresses, leading to smaller overall reinforced areas. Despite the new method resulting in less uniform Puck values across the component, it effectively ensures the component meets the desired fatigue lifetime with less material compared to the more traditional approach.

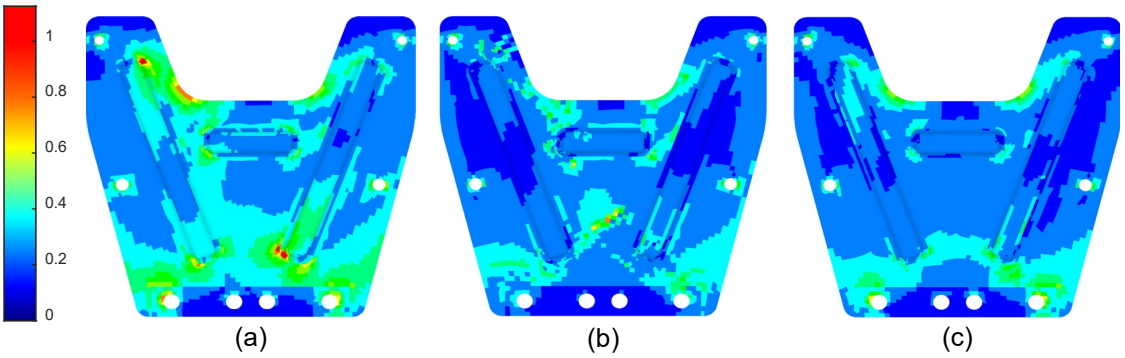

Figure 7: Visualization of the Puck criterion for the non-optimized component (a); for optimization with the new method (b); for static optimization adapted to cyclic loading conditions (c).

6. Summary

The fatigue behaviour of fibre-reinforced composites is highly complex process, influenced by numerous factors. As FRPs find increasing use in critical structural components for mass production, they frequently face cyclic loading. The cyclic stresses lead to the progressive degradation of material properties through the formation and spread of microcracks. Despite this, existing design methods typically overlook the calculation of material fatigue, opting instead for static designs based on one or more failure criteria. By integrating considerations of fatigue due to cyclic loading, it is possible to further enhance the lightweight potential of FRP components, thereby reducing the reliance on substantial safety factors.

An optimization method for the design of fatigue resistant FRP components has been introduced. This method calculates the maximum lifespan of all elements and identifies critical areas using experimentally determined S-N curves in combination with the Puck failure criterion. By locally reinforcing the base laminate, the optimization ensures that a required minimum number of cycles is achieved. The optimization results are then converted into manufacturing-compliant patches, which can be applied to the component using techniques such as FPP. The method was demonstrated in a benchmark showing that FRP components can be automatically optimized for cyclic loading with minimal computational effort. Future work will focus on further enhancing the manufacturability of the resulting patch layers, such as by consolidating smaller patches into larger ones. Furthermore, additional accuracy can be achieved by determining individual b-values of the S-N curves, which have been assumed constant so far. However, since these values are measured on unidirectional single layers, their applicability to layered composites is also to be investigated.

Acknowledgement

The presented research work is funded by the Deutsche Forschungsgemeinschaft (DFG, German Research Foundation) – 508331526 with the title „ZoE – Erforschung der Übertragbarkeit des Zeitfestigkeitsverhaltens bei Faser-Kunststoff-Verbunden von Couponproben auf optimierte Halbzeuge zur Entwicklung einer konstruktionstechnischen Auslegungsrichtlinie“. The authors thank the German Research Foundation for the financial support.

Author Contributions

Conceptualization, C.B. and M.G.; methodology, C.B. and M.G.; software, C.B. and M.G.; validation, C.B. and M.G.; formal analysis, M.G.; investigation, C.B. and M.G.; resources, M.G.; data curation, C.B. and M.G.; writing—original draft preparation, M.G.; writing—review and

editing, C.B., T.D., S.W. and D.K.; visualization, T.D. and M.G.; supervision, S.W. and D.K.; project administration, S.W. and D.K.; funding acquisition, S.W and D.K.

References

[1] Wu, F., Yao, W.: A fatigue damage model of composite materials. In: International Journal of Fatigue Vol. 32 (2010), Nr. 1, pp. 134–138. https://doi.org/10.1016/j.ijfatigue.2009.02.027.

[2] Carraro, P. A., Maragoni, L., Quaresimin, M.: Prediction of the crack density evolution in multidirectional laminates under fatigue loadings. In: Composites Science and Technology Vol. 145 (2017), pp. 24–39. https://doi.org/10.1016/j.compscitech.2017.03.013.

[3] Rajpal, D., Kassapoglou, C., De Breuker, R.: Aeroelastic optimization of composite wings including fatigue loading requirements. In: Composite Structures Vol. 227 (2019), pp. 111248. https://doi.org/10.1016/j.compstruct.2019.111248.

[4] Kussmaul, R. et al.: A novel computational framework for structural optimization with patched laminates. In: Structural and Multidisciplinary Optimization Vol. 60 (2019), Nr. 5, pp. 2073–2091. https://doi.org/10.1007/s00158-019-02311-w.

[5] Bernasconi, A. et al.: Effect of fibre orientation on the fatigue behaviour of a short glass fibre reinforced polyamide-6. In: International Journal of Fatigue Vol. 29 (2007), Nr. 2, pp. 199–208. https://doi.org/10.1016/j.ijfatigue.2006.04.001.

[6] DIN 50100, 2022-12. Schwingfestigkeitsversuch – Durchführung und Auswertung von zyklischen Versuchen mit konstanter Lastamplitude für metallische Werkstoffproben und Bauteile. Berlin, Heidelberg: Beuth. https://doi.org/10.31030/3337109:

[7] Witzgall, C., Gadinger, M., Wartzack, S.: Fatigue Behaviour and Its Effect on the Residual Strength of Long-Fibre-Reinforced Thermoplastic PP LGF30. In: Materials Vol. 16 (2023), Nr. 18, pp. 6174. https://doi.org/10.3390/ma16186174.

[8] VDI 2014: Entwicklung von Bauteilen aus Faser-Kunststoff-Verbund. Düsseldorf: Beuth, 2006:

[9] Ertas, A. H., Sonmez, F. O.: Design of fiber reinforced laminates for maximum fatigue life. In: Procedia Engineering Vol. 2 (2010), Nr. 1, pp. 251–256. https://doi.org/10.1016/j.proeng.2010.03.027.

[10] Fawaz, Z., Ellyin, F.: Fatigue Failure Model for Fibre-Reinforced Materials under General Loading Conditions. In: Journal of Composite Materials Vol. 28 (1994), Nr. 15, pp. 1432–1451. https://doi.org/10.1177/002199839402801503.

[11] Fawaz, Z., Ellyin, F.: A new methodology for the prediction of fatigue failure in multidirectional fiber-reinforced laminates. In: Composites Science and Technology Vol. 53 (1995), Nr. 1, pp. 47–55. https://doi.org/10.1016/0266-3538(94)00077-8.

[12] Deveci, H. A., Artem, H. S.: Optimum design of fatigue-resistant composite laminates using hybrid algorithm. In: Composite Structures Vol. 168 (2017), pp. 178–188. https://doi.org/10.1016/j.compstruct.2017.01.064.

[13] Philippidis, T. P., Vassilopoulos, A. P.: Fatigue Strength Prediction under Multiaxial Stress. In: Journal of Composite Materials Vol. 33 (1999), Nr. 17, pp. 1578–1599. https://doi.org/10.1177/002199839903301701.

[14] Tsai, S. W., Hahn, H. T.: Introduction to Composite Materials. https://doi.org/10.1201/9780203750148, 2018

[15] Voelkl, H., Kießkalt, A., Wartzack, S.: Design for Composites: Derivation of Manufacturable Geometries for Unidirectional Tape Laying. In: Proceedings of the Design Society: International Conference on Engineering Design Vol. 1 (2019), Nr. 1, pp. 2687–2696. https://doi.org/10.1017/dsi.2019.275.

[16] Tsai, S. W., Wu, E. M.: A General Theory of Strength for Anisotropic Materials. In: Journal of Composite Materials Vol. 5 (1971), Nr. 1, pp. 58–80. https://doi.org/10.1177/002199837100500106.

[17] Puck, A.: Festigkeitsanalyse von Faser-Matrix-Laminaten. München, Wien: Hanser, 1996 — ISBN 3-446-18194-6.

[18] Rotem, A., Nelson, H. G.: Failure of a laminated composite under tension—compression fatigue loading. In: Composites Science and Technology Vol. 36 (1989), Nr. 1, pp. 45–62. https://doi.org/10.1016/0266-3538(89)90015-8.

[19] Kawai, M.: A Method for Identifying Asymmetric Dissimilar Constant Fatigue Life Diagrams for CFRP Laminates. In: Key Engineering Materials Vol. 334–335 (2007), pp. 61–64. https://doi.org/10.4028/www.scientific.net/KEM.334-335.61.

[20] ANSYS, Inc: ANSYS Help. https://ansyshelp.ansys.com/account/secured? returnurl=/Views/Secured /main_page.html, Abruf: 08.08.2024.

[21] Klein, D.: Fortschrittberichte VDI : Reihe 1, Konstruktionstechnik, Maschinenelemente. Bd. Nr. 439: Ein simulationsbasierter Ansatz für die beanspruchungsgerechte Auslegung endlosfaserverstärkter Faserverbundstrukturen. Düsseldorf : VDI Verlag GmbH, 2017. – ISBN 978–3–18–343901–0.